The paper was published in the proceedings of the 11th International Conference on Physical Modelling in Geotechnics (ICPMG2026) and was edited by Ioannis Anastasopoulos. The conference was held from June 8th to June 12th 2026 in Zurich, Switzerland.

Proceedings of the 11th ICPMG 2026
11th International Conference on Physical Modelling in Geotechnics
8-12 June 2026, Zurich, Switzerland

Influence of foundation shape and embedment on the dynamic response of the Persefone prototype

T. Lusi
University of Naples Federico II, Naples, Italy, teresa.lusi@unina.it

D. Losanno, F. Silvestri, F. de Silva
University of Naples Federico II, Naples, Italy, daniele.losanno@unina.it, francesco.silvestri@unina.it, filomena.desilva@unina.it

D. Pitilakis
Aristotle University of Thessaloniki, Thessaloniki, Greece, dpitilakis@civil.auth.gr

ABSTRACT: This study shows that soil compliance joint to foundation shape and embedment affect the dynamic response of structures through the outcome of the experimental dynamic identification of a prototype of single degree of freedom system founded on the soft soil of the Euroseistest in Greece. The prototype was designed with a symmetric structure placed on a rectangular footing, in the frame of the project Persefone (Permanent Effects in Rocking Shallow or Embedded Foundations Occurring after Earthquakes). Its dynamic response was identified in both the horizontal directions, considering two configurations for the structural masses (M2, M4) combined with a Shallow (SF) or Embedded (EF) foundation. The accelerations of structure and foundation recorded under ambient noise were analysed both with the Fast Fourier Transform (FFT) and with the Operational Modal Analysis (OMA), which allowed for the identification of the mode shapes. Results confirm that natural frequencies significantly decrease with respect to the values expected for the fixed-based condition, in particular for the configuration on the shallow foundation, along the direction parallel to its shortest side. Finally, the experimental results were compared against analytical predictions obtained through the web application 0D-In. The comparison revealed a close match for the SF configurations, whereas analytical predictions overestimate the experimental frequency values for the EF arrangements, likely due to backfill soil disturbance.

1 INTRODUCTION

Although structures are often designed against earthquakes through fixed-base models, how the structural capacity is mobilized under an earthquake is strictly influenced by the stiffness and the strength of the foundation soil. In particular, soft soil modifies the fundamental period and the damping ratio of structures with respect to the conventional fixed-base assumption, as recognized from records obtained under white noise (Luco and De Barros, 2005; Pitilakis et al., 2018; Star et al., 2019) and weak to strong motions (Luco et al., 1988; Guéguen and Bard, 2005; de Silva et al., 2019; Brunelli et al., 2021). The final effect can be beneficial or detrimental, depending on soil and structural mechanical properties, foundation and building geometry, as well as on the amplitude and the frequency content of the seismic motion.

In literature, only a few full-scale field tests performed on instrumented structures or properly designed prototypes were exploited to evaluate the soil-foundation impedance, the elongation of the fundamental period and the damping ratio of the whole system (Crouse et al., 1984; De Barros and Enrique Luco, 1995; Tileylioglu et al., 2011; Sharma and Deng, 2018, 2021; Amendola et al., 2021). In any case, the structure and the foundation were symmetric and tested in single specific configurations.

This paper reports some preliminary outcomes of full-scale experimental tests aimed to quantify the influence of soil-foundation-structure interaction on the dynamic response of an original prototype, in the frame of the European project *PERSEFONE* (*Permanent Effects in Rocking Shallow or Embedded Foundations Occurring after Earthquakes*).

The goal of the experimental campaign is to characterize the behavior of rocking foundations, specifically investigating the capacity of shallow and embedded foundations to dissipate seismic energy. In particular, the High-amplitude Forced vibration tests allow for the investigation of soil non-linear behaviour and the permanent effects, such as residual settlement, residual rotation, and displacements, occurring after the shaking. The results reported in this paper serve as the preliminary findings necessary for the subsequent interpretation of forced vibration tests.

With respect to the abovementioned similar studies on full scale facilities, this study reports tests on the same symmetric structure on different asymmetric foundation configurations. After a brief description of the designed facility, of the experimental set-up and of the testing programme, the paper focuses on the effect of the foundation width and embedment on the fundamental period as experimentally detected through different numerical techniques.

2 DESIGN AND TESTS OF PERSEFONE

2.1 Description of the Soil-Foundation-Structure system

The PERSEFONE prototype was specifically designed for full-scale tests focusing on the assessment of soil-structure interaction. It was constructed and installed in the EuroProteas test site, located in the Mygdonian Valley in Northern Greece, in the middle of the Euroseistest experimental array (http://euroseisdb.civil.auth.gr). A picture of the structure is shown in Figure 1a.

The subsoil has been extensively characterized through field surface and borehole geophysical investigations, as well as laboratory resonant column and shear strength tests. The results are comprehensively reported by Pitilakis et al. (2018). The foundation soil profile is composed of:

- an uppermost layer of silty clay with sand about 5 m thick.
- a layer of silty sand with local contents of gravel between 5 m and 25 m.
- a layer of marly silt and silty sand down to a depth of 30 m.

The groundwater table lies at a depth of about 1.7 m. The interpretation of the geophysical tests reveals a shear wave velocity of the uppermost 5 m around 100 m/s, and 250 m/s from 5 m up to 30 m.

The prototype is a single-degree-of-freedom system consisting of four vertical steel columns that make the structure symmetric in both directions. The steel columns are 2.20 m high and connected to a fixed reinforced concrete roof slab (0.8 m x 0.8 m x 0.2 m), designed to support up to four additional removable masses (1.4 m x 1.4 m x 0.2 m). The foundation is a rectangular 1.3 m x 0.8 m slab, with a thickness of 0.4 m (Figure 1b-c).

The prototype was designed to be reconfigured by varying both structural and foundation configurations. The first structural configuration, denoted as *M2*, consisted of the fixed slab plus two additional masses, resulting in a total structural height of 3.2 m. In the second configuration, designated as *M4*, the mass was increased by utilizing four more masses (shown in light grey in Figures 1b-c) which extended the total height to 3.6 m. On the other hand, two different foundations configurations were investigated to assess the embedment effect. Firstly, the prototype was tested on a Shallow Foundation (SF), i.e. with the foundation slab positioned directly on the soil surface. Subsequent tests were carried out on an Embedded Foundation (EF) configuration, which required a 0.40 m excavation to achieve a full embedment depth.

A numerical model with the finite element software SAP2000 was developed for both structural configurations, i.e. *M2* and *M4*, assuming fixed-base configuration. Being structurally symmetric, the modal analysis led to a fixed-base frequency, f_0, of 4.54 Hz and 3.33 Hz for *M2* and *M4*, respectively.

2.2 Analytical predictions of the fundamental frequency

The analytical predictions of the system dynamic response were performed using the OD-In web application, developed by de Silva and Silvestri, 2025. This digital tool implements closed-form solutions derived from the *replacement oscillator* model (Veletsos and Meek, 1974) to estimate the equivalent fundamental frequency and the equivalent damping ratio of the soil-foundation-structure system. Specifically, the application computes the natural frequency of the compliant-base system by modelling the structure as being supported by a single or a set of unconnected rectangular footings resting on a viscoelastic half-space, whose impedance functions are derived from the analytical solutions by Pais and Kausel (1988). The underlying formulation overcomes the limitations of traditional circular footing approximations by explicitly accounting for the foundation aspect ratio, i.e. L/B, and the number of footings. Furthermore, the tool incorporates correction factors to account for the foundation embedment.

The natural frequencies, f^*_{an}, were computed for the four configurations, *SF-M2, SF-M4, EF-M2,* and *EF-M4*, considering the fixed-base period defined beforehand, the structural height, and the total inertial mass of the upper slabs. The results are listed in Table 1.

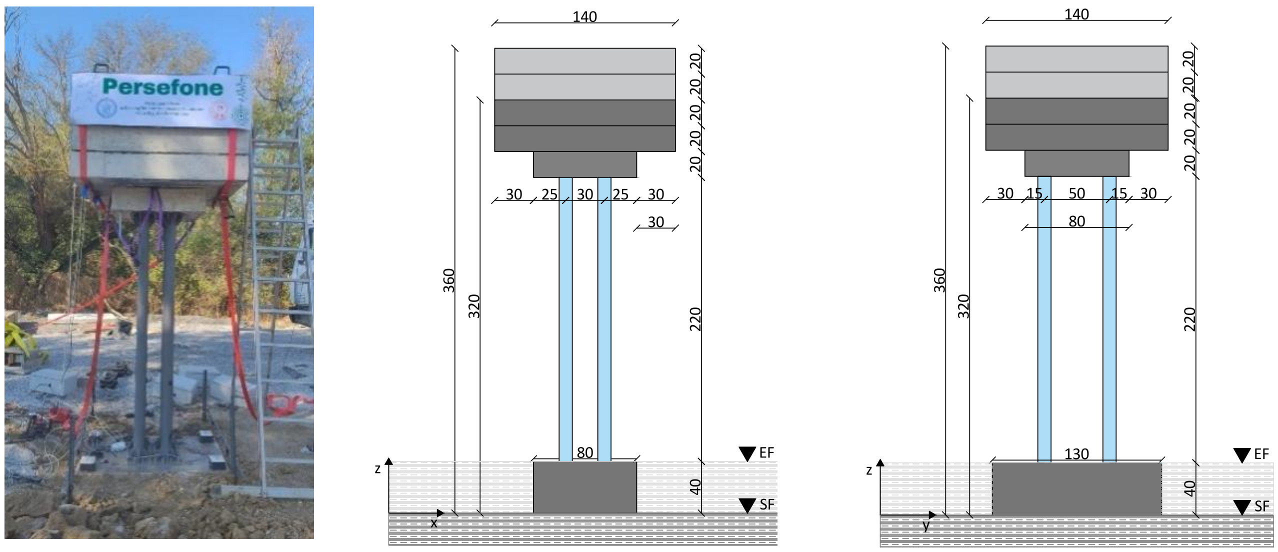

(a) (b) (c)

Figure 1. Persefone facility: (a) on-site photograph of the prototype in EF-M2 configuration, cross sections in the z-x plane b) and in z-y plane c). In (b) and (c) the additional slabs for the M4 configuration are shown in light grey, while the dashed black line indicates the embedment depth for EF configurations (dimensions in cm).

Table 1. Analytical and experimental natural frequencies for SF-M2, SF-M4, EF-M2, and EF-M4 configurations

Configuration [-]	Mode [-]	f^*_{an} [Hz]	f^*_{FFT} [Hz]	f^*_{FDD} [Hz]
SF – M2	1° (x dir)	2.33	2.35	2.38
	2° (y dir)	2.91	2.93	2.93
	3°(z dir)		4.46	4.44
SF – M4	1° (x dir)	1.67	1.77	1.70
	2° (y dir)	2.09	2.14	2.12
	3°(z dir)		3.23	3.23
EF – M2	1° (x dir)	3.18	2.78	2.78
	2° (y dir)	3.15	3.04	3.03
	3°(z dir)		4.49	4.49
EF – M4	1°(xy dir)	2.32	2.12	2.19
	2° (yx dir)	2.56	2.17	2.24
	3° (z dir)		3.25	3.22

2.3 Full-scale tests

The experimental campaign investigated the system's dynamic response across a wide range of excitation levels through three distinct protocols:

- Low-amplitude Forced vibration tests (LF) to quantify the dynamic soil-foundation impedance functions.
- High-amplitude Forced vibration tests (HF) to quantify likely permanent effects.
- records of the soil-structure system response under random ambient noise, acquired before and after each forced vibration test, in the absence of any external excitation.

Tests LF were executed by exciting the structure on the top through the APS-420 electric shaker which applies a force amplitude equal to 1 kN independently of the frequency. Conversely, in the HF tests, the MK-500U eccentric mass shaker was adopted to apply higher forces.

2.4 Instrumentation layout

Figure 2 shows the layout of the instruments designed to monitor the dynamic response of the SFS system. The motion of the prototype was recorded using six triaxial accelerometers (ETNA-2) with a sampling frequency set to 200 Hz, installed at the corners of the slabs to capture both translational and rotational modes. Specifically, four sensors were placed on the foundation and two on the uppermost roof slab. The vertical displacements of the foundation slab were monitored using four laser displacement sensors (Waycon). Additionally, to characterize the soil response and the wave propagation in the near-field, four triaxial seismometers (CMG-40) were deployed on the soil surface surrounding the prototype. Two sensors were arranged along the x direction and two along the y direction. In both cases, the seismometers were placed at distances of 0.8 m and 1.6 m from the prototype.

Data acquired from the different sensor types, except for the laser sensors, were synchronized to share a common initial timestep, through connection to external Global Positioning System (GPS) antennas. The raw data were processed using the Seismic Analysis Code (SAC) software. A baseline correction was applied to all records, consisting of the removal of the mean value and of a linear trend, before conversion to physical engineering units.

3 SYSTEM IDENTIFICATION METHODS

3.1 Experimental evidence

The ambient noise recordings were processed using two distinct approaches: the single-signal processing of each component recorded by the triaxial accelerometers and the Operational Modal Analysis (OMA).

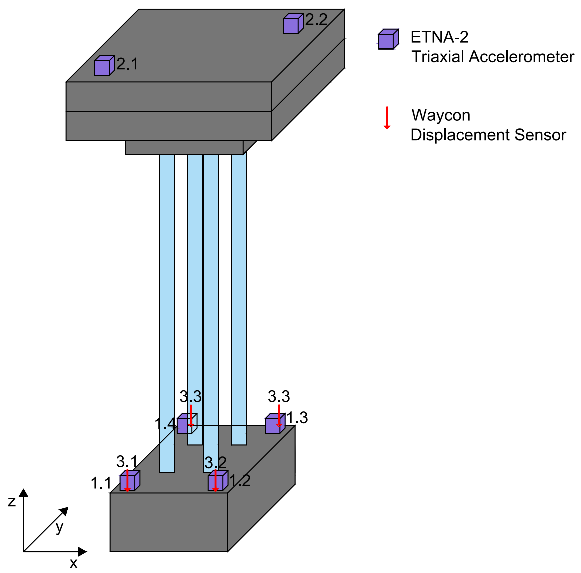

Figure 2. Instrumentation layout for response monitoring: setup of six ETNA-2 triaxial accelerometers (1.1, 1.2, 1.3, and 1.4 on the foundation and 2.1 and 2.2 on the roof), and four Waycon laser displacement sensors ahead each ETNA (3.1, 3.2, 3.3, and 3.4)

3.1.1 Single-signal spectral analysis

The horizontal components of the roof TXA 2.1 and 2.2 were transformed into the frequency domain using the Fast Fourier Transform (FFT) algorithm. This process yielded the Fourier Amplitude Spectra (FAS) for each test configuration, in both horizonal direction. In Figures 3a-c and Figures 4a-c, the FAS is plotted against frequency for x direction and y direction, where the peaks define the resonance frequency, f^{*}_{FFT}, in the corresponding direction. The identified peaks are reported in Table 1.

Independently of the direction and of the inertial mass, the plots highlight a peak close to the fixed-base natural frequency of the system, occurring at approximately 4.5 Hz for M2 and 3.3 Hz for M4 configuration. In any case, additional ranges of significant amplification can be distinguished at lower frequencies. The identification of the vibration modes associated with those frequencies was carried out through the Operational Modal Analysis (OMA) described in the following.

3.1.2 Operational Modal Analysis

The dynamic identification of the global response of the system, in terms of natural frequencies, damping ratios and mode shapes, was obtained processing the ambient noise records through an Operational Modal Analysis (Rainieri, 2014). This was performed by means of ARTeMIS software suite, adopting a Frequency Domain Decomposition (FDD) technique which assumes the structure as linear, time-invariant, and subjected to uncorrelated excitation.

The software requires uploading each recorded signal and defining the position of the measurement points representing the degrees of freedom of the model. The FDD method applies a Singular Value Decomposition (SVD) to the Power Spectral Density (PSD) matrix, G_{yy}, estimated via the Welch procedure (Brincker et al., 2001).

Adopting the standard peak-picking approach (Losanno et al., 2013), modal frequencies were identified from the peaks of the first singular value curve, while mode shapes were extracted from the corresponding singular vectors. Figures 3b-d and Figures 4b-d report the PSD of the first singular vector for SF and EF, respectively, the peak values of which, f^{*}_{FDD}, are reported in Table 1.

The mode shapes identified in this way revealed that, in general, the first and the second peaks correspond to the translational modes in the x and y directions, respectively (Figures 5a-b), while the third peak represents a torsional mode (Figure 5c). This behavior is clearly identifiable for the *SF-M2*, *SF-M4*, and *EF-M2* configurations. However, for the *EF-M4* configuration, the system dynamic response is modified by the combined effect of the increased structural mass and soil embedment. In this case, the experimental data show modal coupling. As a result, the translational components are no longer independent, and the mode shapes exhibit a coupled behaviour in the two directions, as depicted in Figure 5d. This effect explains why the PSD of the first singular value for *EF-M4* have only two dominant peaks instead of three, the first around 2.2 Hz and the second around 3.22 Hz. However, by analysing the second SVD, not reported herein, which allows the identification of closely spaced modes, an additional peak close to the first one is found around 2.24. This is attributed to the fact that the mode shapes associated with these closely spaced frequencies, i.e. 2.19 Hz and 2.24 Hz, exhibit coupled behaviour, as shown in Figure 5d.

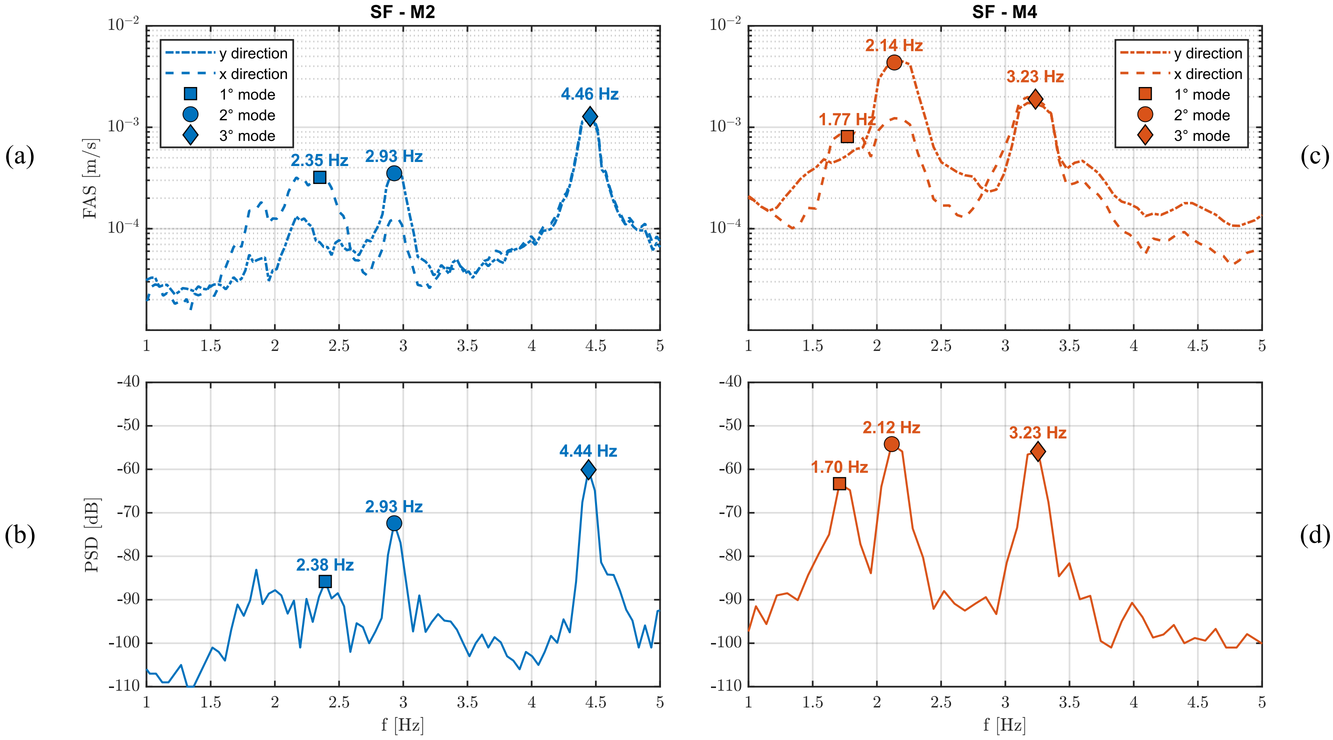

Figure 3. Shallow Foundation model: FFT for SF-M2 (a) and for SF-M4 (c) configurations, along both x and y directions; PSD of the first SVD for SF-M2 (b) and for SF-M4 (d).

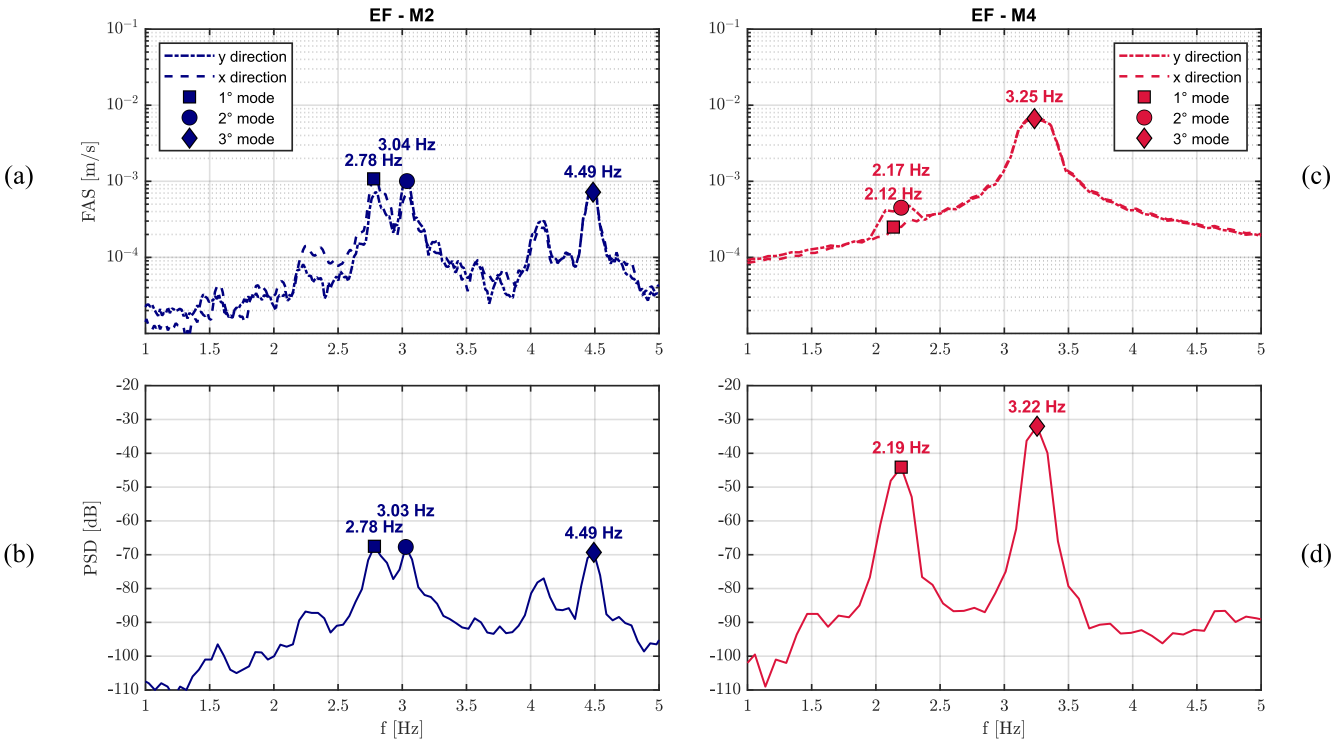

Figure 4. Embedded Foundation model: FFT for EF-M2 (a) and for EF-M4 (b) configurations along both x and y directions; PSD of the first SVD for EF-M2 (b) and for EF-M4 (d).

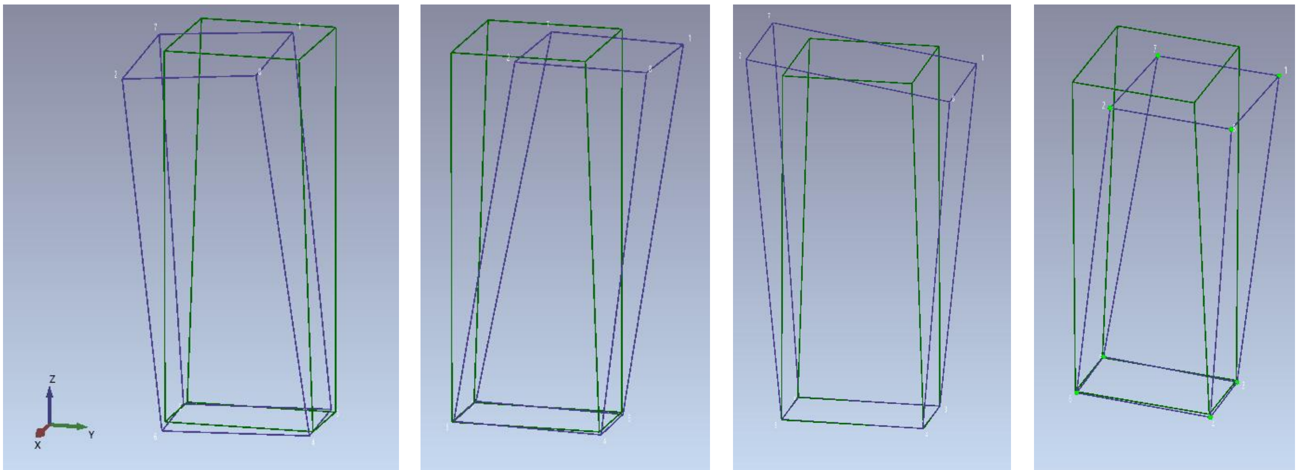

(a) (b) (c) (d)

Figure 5. Mode shapes for configuration SF-M2, SF-M4 and EF-M2: (a) 1° mode, x direction; (b) 2° mode, y direction; (c) 3° mode, torsional. (d) 1° coupled mode shape for configuration EF-M4.

In general, the fundamental frequencies are lower than the expected fixed-base values. The reduction is more significant for the configuration on shallow foundation, being maximum in the direction parallel to the shortest foundation side. Conversely, the influence of geometric asymmetry, which typically separates the natural frequencies in the two principal directions, is reduced by soil embedment and the increase in structural weight.

3.2 Comparison

The frequencies for each configuration and along the two horizontal directions are summarised in Table 1.

The experimental values, derived from both the single-signal spectral analysis of the roof sensor and from the application of the OMA, demonstrate a very good agreement with the analytical predictions. It should be noted, however, that the third vibration mode was identifiable exclusively through experimental data.

The experimental frequencies, f^*_{FDD}, are plotted in Figure 6a-c for each configuration, against the number of additional masses. As expected, for both the shallow and embedded foundation, increasing the structural weight leads to a reduction in frequency, as the structural stiffness remains unvaried.

Conversely, when the foundation is embedded, the system stiffness increases, resulting in higher natural frequencies. It should be noted that the difference between the *EF* and the *SF* models is less pronounced in the y direction. This behaviour likely arises because the system is inherently stiffer in the y direction; consequently, the stiffening effect provided by soil embedment is less significant compared to the x direction.

In Figure 6b-d the experimental frequencies, f^*_{FDD}, are compared to the analytical values, f^*_{an}. For the shallow foundation configurations, *SF-M2* and *SF-M4*, the analytical frequencies closely match the experimental ones. Specifically, regarding the *SF-M4* configuration, the experimentally determined frequencies for the first two modes appear slightly higher than the analytical values, indicating a stiffer system response. This phenomenon is likely attributable to the chronological sequence of the experimental program: the high-amplitude forced vibration tests conducted on the preceding configurations may have induced a stiffening of the soil, leading to a slight increase in its shear wave velocity, V_s. Conversely, the embedded configurations, *EF-M2* and *EF-M4*, reveal an overestimation in the analytical frequencies. This implies that the analytical formulation assumes a stiffer behaviour than that observed in situ.

This discrepancy is likely caused by the disturbance of the backfill soil during the excavation process, which may have resulted in a local reduction of the shear wave velocity.

4 CONCLUSIONS

The dynamic identification executed on a full - scale prototype structure of single degree of freedom system confirmed that the fundamental frequency is lower than the value calculated through a fixed-base model. The reduction is more significant for shallow foundations and along the direction x, that is parallel to the shortest side of the foundation.

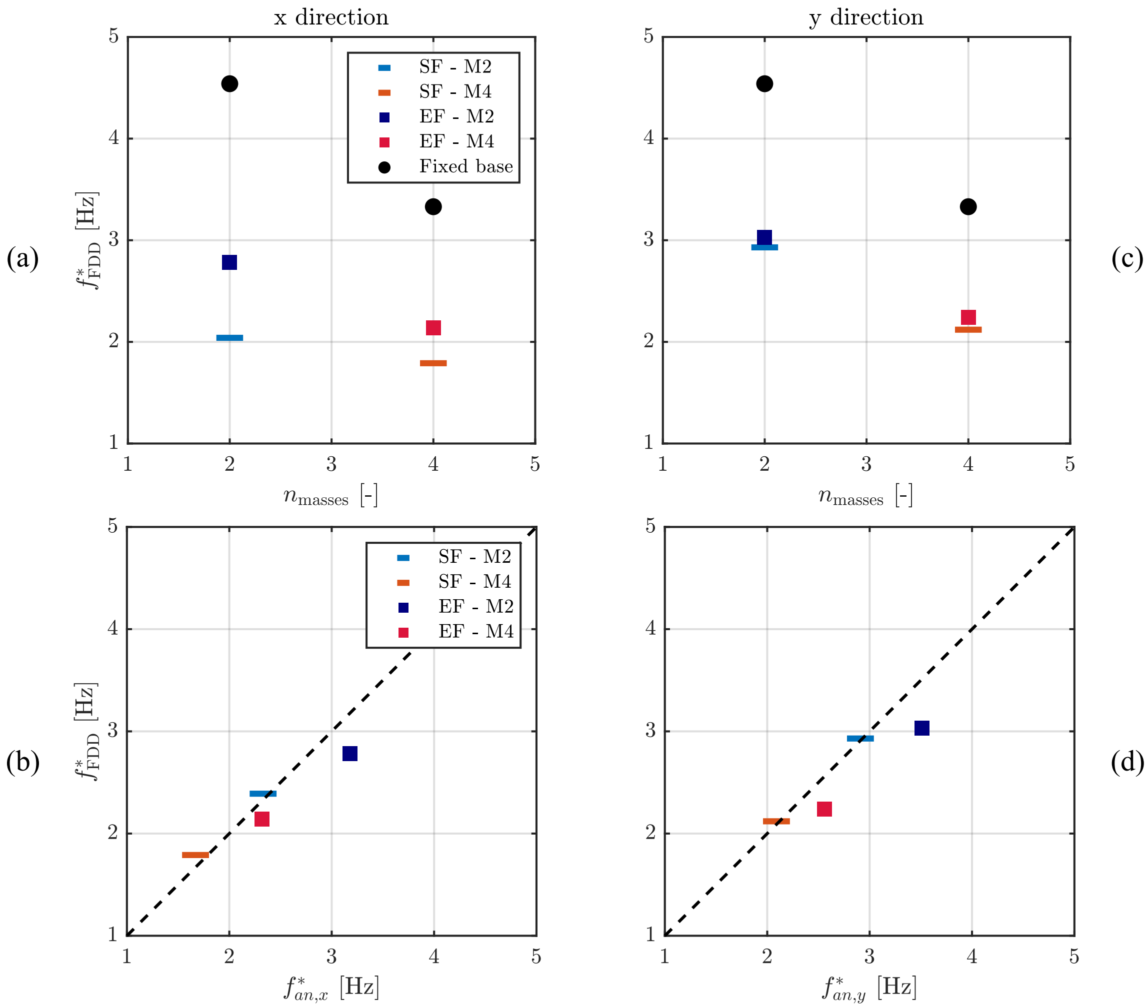

Figure 6. Experimental and fixed-base natural frequencies in x (a) and y direction (c) vs. the number of structural masses; experimental natural frequency compared to the analytical predictions in x (b) and y direction (d).

The foundation embedment produces the expected stiffening of the soil-foundation system leading to an increase of the structural fundamental frequency with respect to the case on shallow foundation, but such increase is again more important along the x-direction.

The experimental values are in a satisfying agreement with the analytical predictions for the shallow foundation. The estimation for the case on embedded foundation is generally higher with respect to the experimental evidence, probably due to the reduced shear stiffness of the backfill that the analytical model cannot account for.

Finally, the experimental results show that the combined effect of the increased structural mass and soil embedment generates modal coupling in the two directions.

In conclusion, the dynamic identification performed on the full-scale prototype Persefone defines the system dynamic properties necessary to the interpretation of the forced vibration tests.

ACKNOWLEDGEMENTS

The authors acknowledge support by the project *Engineering Research Infrastructures for European Synergies*, *ERIES*.

This project was funded under the grant agreement No. 101058684 with the European Commission. The results of this research will be also exploited in the framework of the 2024–2026 ReLUIS-DPC research programme funded by the Italian Civil Protection Department, as a contribution to the geotechnical Work Package 'Soil-Foundation-Structure Interaction' (Task 16.2).

REFERENCES

Amendola, C., de Silva, F., Vratsikidis, A., Pitilakis, D., Anastasiadis, A., Silvestri, F., 2021. Foundation impedance functions from full-scale soil-structure interaction tests. Soil Dynamics and Earthquake

Engineering 141, 106523. https://doi.org/10.1016/j.soildyn.2020.106523

Brincker, R., Zhang, L., Andersen, P., 2001. Modal identification of output-only systems using frequency domain decomposition. Smart Mater. Struct. 10, 441–445. https://doi.org/10.1088/0964-1726/10/3/303

Brunelli, A., de Silva, F., Piro, A., Parisi, F., Sica, S., Silvestri, F., Cattari, S., 2021. Numerical simulation of the seismic response and soil–structure interaction for a monitored masonry school building damaged by the 2016 Central Italy earthquake. Bull Earthquake Eng 19, 1181–1211. https://doi.org/10.1007/s10518-020-00980-3

Crouse, C.B., Liang, G.C., Martin, G.R., 1984. Experimental study of soil-structure interaction at an accelerograph station. Bulletin of the Seismological Society of America 74, 1995–2013. https://doi.org/10.1785/BSSA0740051995

De Barros, F.C.P., Enrique Luco, J., 1995. Identification of foundation impedance functions and soil properties from vibration tests of the Hualien containment model. Soil Dynamics and Earthquake Engineering 14, 229–248. https://doi.org/10.1016/0267-7261(94)00046-J

de Silva, F., Piro, A., Brunelli, A., Cattari, S., Parisi, F., Sica, S., Silvestri, F., 2019. On the soil-structure interaction in the seismic response of a monitored masonry school building struck by the 2016-2017 Central Italy earthquake. COMPDYN 2019. Proc. 7th ECCOMAS Thematic Conference on Computational Methods in Structural Dynamics and Earthquake Engineering. Crete, Greece, pp. 1853–1862. https://doi.org/10.7712/120119.7041.19395

de Silva, F., Silvestri, F., 2025. Derivation, Validation, and Web Application of Dimensionless Analytical Solutions for Equivalent Period and Damping Ratio of Soil-Foundation-Structure Systems. J. Geotech. Geoenviron. Eng. 151, 04025049. https://doi.org/10.1061/JGGEFK.GTENG-12927

Guéguen, P., Bard, P.-Y., 2005. Soil-structure and soil-structure-soil interaction: experimental evidence at the Volvi test site. Journal of Earthquake Engineering 9, 657–693. https://doi.org/10.1080/13632460509350561

Losanno, D., Londono, J.M., Spizzuoco, M., 2013. Structural monitoring system for the management of emergency due to natural events, in: 2013 IEEE Workshop on Environmental Energy and Structural Monitoring Systems. Trento, Italy, pp. 1–6. https://doi.org/10.1109/EESMS.2013.6661703

Luco, J.E., De Barros, F.C.P., 2005. Identification of structural and soil properties from vibration tests of the Hualien containment model. Earthquake Engng Struct. Dyn. 34, 21–48. https://doi.org/10.1002/eqe.404

Luco, J.E., Trifunac, M.D., Wong, H.L., 1988. Isolation of soil-structure interaction effects by full-scale forced vibration tests. Earthq Engng Struct Dyn 16, 1–21. https://doi.org/10.1002/eqe.4290160102

Pais, A., Kausel, E., 1988. Approximate formulas for dynamic stiffnesses of rigid foundations. Soil Dynamics and Earthquake Engineering 7, 213–227. https://doi.org/10.1016/S0267-7261(88)80005-8

Pitilakis, D., Rovithis, E., Anastasiadis, A., Vratsikidis, A., Manakou, M., 2018. Field evidence of SSI from full-scale structure testing. Soil Dynamics and Earthquake Engineering 112, 89–106. https://doi.org/10.1016/j.soildyn.2018.04.024

Rainieri, C., 2014. Operational Modal Analysis of Civil Engineering Structures: An Introduction and Guide for Applications, 1st ed. ed. Springer New York, New York, NY.

Sharma, K., Deng, L., 2021. Effects of loading obliquity on field performance of rocking shallow foundations in cohesive soil. Géotechnique 71, 320–333. https://doi.org/10.1680/jgeot.19.P.033

Sharma, K., Deng, L., 2018. Field Experiment of Rocking Shallow Foundation on Cohesive Soil Subjected to Lateral Cyclic Loads, in: Geotechnical Earthquake Engineering and Soil Dynamics V. Presented at the Geotechnical Earthquake Engineering and Soil Dynamics V, American Society of Civil Engineers, Austin, Texas, pp. 379–387. https://doi.org/10.1061/9780784481479.039

Star, L.M., Tileylioglu, S., Givens, M.J., Mylonakis, G., Stewart, J.P., 2019. Evaluation of soil-structure interaction effects from system identification of structures subject to forced vibration tests. Soil Dynamics and Earthquake Engineering 116, 747–760. https://doi.org/10.1016/j.soildyn.2018.09.038

Tileylioglu, S., Stewart, J.P., Nigbor, R.L., 2011. Dynamic Stiffness and Damping of a Shallow Foundation from Forced Vibration of a Field Test Structure. J. Geotech. Geoenviron. Eng. 137, 344–353. https://doi.org/10.1061/(ASCE)GT.1943-5606.0000430

Veletsos, A.S., Meek, J.W., 1974. Dynamic behaviour of building-foundation systems. Earthq Engng Struct Dyn 3, 121–138. https://doi.org/10.1002/eqe.4290030203